One-year stability of glucose dehydrogenase confined in a 3D carbon nanotube electrode with coated poly-methylene green: Application as bioanode for a glucose biofuel cell

Awatef Ben-Tahar, Anthony Szymczyk, Sophie Tingry, Pankaj Vadgama, M. Zelsmann, Seiya Tsujumura, Philippe Cinquin, Donald Martin, Abdelkader Zebda

One-year stability of glucose dehydrogenase confined in a 3D carbon Nanotube electrode with coated Poly-Methylene Green: application as bioanode for a glucose biofuel cell

A. Ben Tahar[1], A. Szymczyk[2], S. Tingry[3], P. Vadgama[4], M. Zelsmann[5], S. Tsujumura[6], P. Cinquin[1], D. Martin[1], A. Zebda[1]

[1]UGA-Grenoble 1 / CNRS / INSERM / TIMC-IMAG UMR 5525, Grenoble, 38000, France

[2]Univ Rennes, CNRS, ISCR (Institut des Sciences Chimiques de Rennes) – UMR 6226, F-35000 Rennes, France

[3]Institut Européen des Membranes, UMR 5635, ENSCM-UMII-CNRS, place Eugène Bataillon, 34095 Montpellier, France

[4]Queen Mary University of London, Mile And Road, E14N, London, United Kingdom

[5]Laboratoire des Technologies de la Microélectronique, LTM-CNRS-UJF, CEA-LETI, 17 av. des Martyrs, 38054 Grenoble, France

[6]Faculty of Pure and Applied Sciences, University of Tsukuba, 1-1-1 Tennodai, Tsukuba, Ibaraki 305-8573, Japan

Abstract

We report a new approach to fabricate an efficient 3D glucose bioanode based on the co-immobilization of the enzyme glucose dehydrogenase (GDH), its cofactor NADP, and Multiwall Carbon Nanotubes (MWCNTs) coated with poly (Methylene Green) (PMG). The MWCNT-PMG composite was obtained by chemical polymerization of Methylene Green (MG) monomer on the MWCNT surfaces. Structural and chemical analyses clearly showed successful coating of the MWCNTs with PMG that markedly affected their morphological and surface charge properties. Electrochemical investigation of PMG-MWCNTs mixed with GDH and NADP showed high stability with extended bioanode electrocatalytic activity towards glucose oxidation for more than one year.

I. Introduction

In recent years, considerable effort has been made to advance a new generation of enzymatic electrochemical systems to serve variously as implantable biosensors and biofuel cells [1,2]. These devices are typically based on glucose utilization and offer a promising route to *in vivo* glucose monitoring in diabetes or to supply energy for active, implantable, medical devices such as pacemakers and insulin pumps [3,4]. For glucose enzyme electrodes, the most exploited enzymes are glucose oxidase (GOx) and glucose dehydrogenase (GDH) [5]. Currently, successful commercial glucose biosensors generally use these two enzymes, but for *in vivo* applications, GOx has major drawbacks due to dependence on O_2 co-substrate and the production of a cell toxic reaction product – H_2O_2 [1,4]. The local buildup of H_2O_2 has potential for high toxicity, even though the overall small quantities generated are unlikely to lead to general toxic effects because of catalase in the body. For these reasons, and in view of the need for *in vivo* application, GDH is an attractive alternative; its requisite cofactors, notably NAD^+ and $NADP^+$ pose no toxicity outcomes as electron acceptors for glucose [6]. However, the desired electrode needs to be able to recycle $NAD^+/NADP^+$ without electrode surface passivation or poisoning, and in particular to exhibit NAD(P)H oxidation at low polarizing voltage [7,8]. The challenge with unmodified electrodes is to overcome kinetically impeded electron transfer, which is the key factor responsible for obligatory significant overpotentials greater than the equilibrium potential of the $NAD(P)H/NAD(P)^+$ couple of -320 mV (*vs*. NHE) typically required [7,8,9]. Furthermore, the large overvoltage demanded for NADH oxidation at traditional electrodes leads to cumulative formation of nicotinamide dimers fouling the electrode surface which in turn results in unreliable responses [9,10].

Therefore, considerable effort has been devoted to new and modified electrode surfaces capable of catalyzing the oxidation of NAD(P)H–at low potentials [11] without surface passivation. Whilst a variety of alternative NADH regeneration approaches are available:

biological, chemical, photochemical, electrochemical and enzymatic [11,12], they all add a further level of complexity, and as conFigd do not generate an electrode current directly. An effective electrochemical regeneration method remains an attractive goal for glucose monitoring, not least given the integral role it has within the transduction process. Organic mediators such as methylene green (MG), methylene blue (MB) and neutral red (NR) are well known to oxidize NADH efficiently in either monomer or polymer form [13]. Minteer *et al* [14a] investigated the effect of both chemical and electrochemical polymerization of some of these monomers on their capacity to oxidize NADH. These kinetic studies showed that chemically synthesized Poly(MG) (PMG) exhibits a catalytic constant k_{cat} (turnover number), three times greater than any other polymer studied - including electrochemically synthesized forms. However, when used for practical electrocatalysis in a methanol biofuel cell, chemically synthesized polymer showed only similar performance to electrochemically synthesized polymers due to significant transport limitation observed during bioanode operation. In another study, Minteer *et al* [14b] succeeded in employing various electro-polymerized Azine-based NADH electrocatalysts onto carbon nanotube surfaces. The electro-polymerization procedure did not deactivate the GDH enzyme, and highest performance here was achieved with PMG.

The role of CNTs in enhancing the efficiency of the electropolymerized Azine was additionally demonstrated by Barton *et al* [15] who showed higher NADH oxidation rates on carboxylated carbon nanotubes surfaces with electrodeposited PMG (PMG-CNT) than poly(toluidine blue) (PTBO-CNT), especially at high NADH concentration and overpotential. However, like the majority of these enzymatic bioelectrodes suffer from limited stability due to the short operational lifetime of the enzyme GDH; this precludes *in vivo* use. In our previous work, we demonstrated that the incorporation of laccase and GOx within 3D MWCNT pellets allows the creation of more favorable environment for enzymes and the

resulting enzymatic bioelectrodes exhibited long-term stability, extending over several months [16, 17]. Indeed, a laccase incorporated MWCNTs-chitosan composite exhibited stability of up to 4 months under *in vitro* storage condition and more than 2 months under *in vivo* conditions [18]. These studies clearly show that 3D MWCNTs offer a significant advantage for enzymatic electrode stabilization. However, to develop a GDH based 3D MWCNT bioanode pellet, both GDH and its cofactor NADP need to be incorporated into the composite, along with PMG to regenerate NADP efficiently.

In the case of a 3D MWCNT pellet, the electropolymerization of MG is challenging because of the likely limited diffusion of the MG molecule through the pellet pores. Moreover, homogeneous deposition of PMG is unlikely, given that growth at the surface will occur more quickly than within the bulk.

In this study, we report a GDH based 3D bioanode that for the first time secures long-term stability of the enzyme. In this bioanode, GDH and its cofactor NADP were confined within a 3D MWCNT-PMG porous matrix, obtained by chemical polymerization of MG onto the MWCNT surface. This composite provided a non-toxic source material for the elaboration of the 3D bioanode and enzyme incorporation, and ensured stability during extended storage. To achieve this, the pre-formed MWCNT-PMG composite was mixed with GDH and NADP in a separate step and then compressed with additional binder to obtain the 3D pellet bioanode. Electrochemical studies demonstrated that this bioanode exhibited high, sustained, electrocatalytic activity toward glucose with an enzyme stability of over one year. The morphology of the electrode material, its surface area and its surface charge properties are also presented along with a suggested mechanism for the enhanced operational performance and favorable enzyme stability.

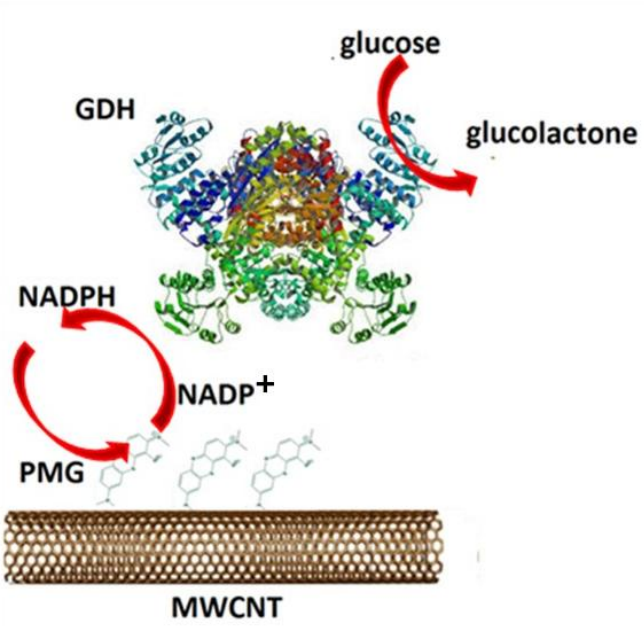

Schematic 1: Representation of the enzymatic reaction cascade mechanism on the surface of a PMG coated MWCNT electrode

2. Materials and methods

2.1 Enzyme and chemicals

Methylene green (MG), and Nafion solution (5%) were purchased from Sigma-Aldrich (Saint Quentin Fallavier, France). Nicotinamide adenine dinucleotide phosphate (NADP) and glucose dehydrogenase (GDH) from microorganism (E.C. 1.1.1.47) were purchased from Sorachim Switzerland. Phosphate Buffer Saline (PBS) tablets (0.01 mol L^{-1},0.14 mol L^{-1} NaCl, 0.0027 mol L^{-1} KCl, pH 7.4) were purchased from Euromedex (Souffelweyersheim, France). Silicone (AS310) was purchased from SILICOMET France. All aqueous solutions were prepared using ultrapure water from a Millipore system. Commercial-grade thin MWCNTs (9.5 nm diameter, purity > 95 %,) were obtained from Nanocyl Belgium. All of the chemicals used were of analytical grade and used without further purification.

2.2 Chemical synthesis of PMG coated MWCNT

MWCNT-PMG composite was chemically synthesized using a protocol described by Minteer *et al* [14]. MWCNTs (150 mg), MG monomer (28 mg), water (91.7mL) and concentrated HCl (8.3mL) were mixed and cooled in a dry-ice bath overnight. This was followed by the addition of 0.81 g of Fe (III) chloride. The resulting polymer coating was washed with vacuum filtration using successive rinses of 1M hydrochloric acid, 1M ammonia, 1-methyl-2-pyrrolidone, methanol, and diethyl ether. This protocol resulted in a MWCNT-PMG solid product that appeared dark green to almost black. The resulting product was rinsed for a further 40 hours in water and then centrifuged for 5 min at 3500 rpm to eliminate residues of the monomer.

2.2 Bio-electrode designs

2.3 .1 Bioelectrode based on carbon paper

A suspension of MWCNT-PMG was prepared as an ink by the addition of 2 mL of water containing 0.375% of dodecyl sulfate sodium (SDS) to 5mg of MWCNT-PMG and the mixture sonicated for 30 min. The presence of SDS in the aqueous suspension is intended to improve the dispersion of MWCNTs-PMG and to obtain a homogeneous ink. Then 100 µL of the prepared ink was in turn deposited on the carbon paper surface (0.5 cm^2) and left to dry for 60 min at room temperature. We deposited on the MWCNTs-PMG, 150 µL solution 5% Nafion (prepared using Minteer *et al* protocol [19]) containing GDH (2.5 mg/mL) and NADP (20 mg/mL) and allowed to dry for 60 min at room temperature.

2.3.2 Bioelectrode based on a 3D pellet

A 200 µL mixture of GDH (4 mg), $NADP^+$ (15 mg), MWCNTs/PMG (25 mg) and viscous Nafion (using the method of Minteer *et al* [19]) was used to prepare a compacted disk (surface: 0.2 cm^2, thickness: 3 mm) using a manual press. In order to set up the electrical

connection, a copper wire was embedded in the carbon paste covering one side of the disk. The perimeter and the covered side of the disc were isolated with silicone. The resulting bioanode was dried at ambient temperature for 12 h and then stored at 4°C until use in PBS buffer solution.

2.4. BET Surface Area of Porous Carbon

The surface area of the bioanode pellets was determined by Brunauer–Emmett–Teller (BET) measurements: N_2 adsorption–desorption isotherms were acquired using a Micromeritics ASAP 2020 instrument. The samples were previously degassed at ambient temperature for 2 h. Average pore size distribution was calculated *via* the Barrett-Joynes-Halenda (BJH) method [22].

2.5 The Field-emission gun scanning electron microscopy (FEG–SEM)

The structure of the bio-electrode was characterized by FEG-SEM using an ULTRA 55 FESEM based on the GEMENI FESEM column (Nanotechnology Systems Division, Carl Zeiss NTS GmbH). Samples were sputtter-coated with 1 nm gold-palladium using a precision etching coating system (PSCE 682- Gatan, Inc., CA).

2.6 Zeta potential determination

Streaming potential is an attractive technique allowing the characterization of the surface electro-kinetic properties of solids with various shapes and geometries [23, 24]. The porous plug method was used in this work [22].

All measurements were performed with a SurPASS electrokinetic analyzer (Anton Paar GmbH). MWCNTs and MWCNTs-PMG were first immersed in the measuring solution for 24 hours. Porous plugs were further formed by compressing a given amount (c.a. 35 mg) of

MWCNTs or MWCNT-PMG between two Ag/AgCl electrodes placed on either side of the porous plug. The measuring solution was circulated through the electrodes and MWCNT porous plug for about one hour (equilibration step). The streaming potential was then measured with the Ag/AgCl electrodes by applying hydrostatic pressure differences of up to 600 mbar through the porous plug. Measurements were performed for pH values ranging from c.a. 9.5 to 2.5 using the automatic titration unit associated with the SurPASS instrument. Streaming potential measurements were followed by a Fairbrother-Mastin correction procedure (measurement of the electrical resistance of the porous plug at high concentration) in order to take into account the impact of the surface conductance on the streaming potential[20]. Streaming potential measurements were carried out with millimolar KCl solutions while a decimolar KCl solution was used for the Fairbrother-Mastin correction procedure. All measurements were performed at room temperature (22 ± 1 °C).

2.7 Electrochemical measurements

A BILOGIC Instruments 650 potentiostat interfaced to a PC was used for all experiments along with a saturated calomel electrode (SCE) as reference and a platinum mesh as the counter electrode, unless otherwise stated. The bioelectrodes based on carbon paper and Those based 3D pellet were employed as the working electrodes. To evaluate the electrochemical properties of the composites, the MWCNTs-PMG modified carbon electrodes were equilibrated in 10mM pH 7.4 phosphate buffer. Cyclic voltammograms were obtained at a scan rate of 1 mV/s. The potential window used was −1.0 to 1.0V *vs* SCE.

The chronoamperometric response of the bio-electrodes was recorded at +0.150 V *vs* SCE. All measurements were performed at ambient temperature (20 ± 3°C).

To evaluate the stability of the bioelectrode disks, periodic chronoamperometric measurements were taken daily during the first five days and later at different time intervals.

After each measurement, the bioelectrode disks were stored for 60 days at 4°C under dry conditions.

2.8 Spectrophotometric measurements

GDH activity was monitored by measuring the reduction of NADPH to NADP determined by the increase in absorbance at : 340 nm with an extincting coefficient of 6200 $M^{-1}cm^{-1}$ for NADPH and at 260 nm with an extincting coefficient of 17800 $M^{-1}cm^{-1}$ for NADP [25]. The reaction mixture contained PBS buffer, 20 mM substrate (NADP), 50 mM glucose. Measurements were performed with Spectrophotometer Beckman DU®530. Enzyme activity was expressed in µmol of NADP reduction per minute. The enzyme activity was monitored using sample volumes from the anode buffer storage.

Results and discussion

3.1. Morphology

As observed in the FEG-SEM images shown in Fig 2, the chemical polymerization procedure led to a major modification to the morphology of the pristine MWCNTs whose diameters increased from 10 nm (Fig.2A) to 100 nm (Fig.2B). The MWCNT-PMG composite disc exhibits heterogeneous organization resulting from the non-uniform deposition of PMG on the outer layer of the MWCNTs caused by the limited dispersion of MWCNTs in the polymerization solution. These results are confirmed by TEM observations, which depict the formed coatings onto the MWCNTs (see in supplementary information).

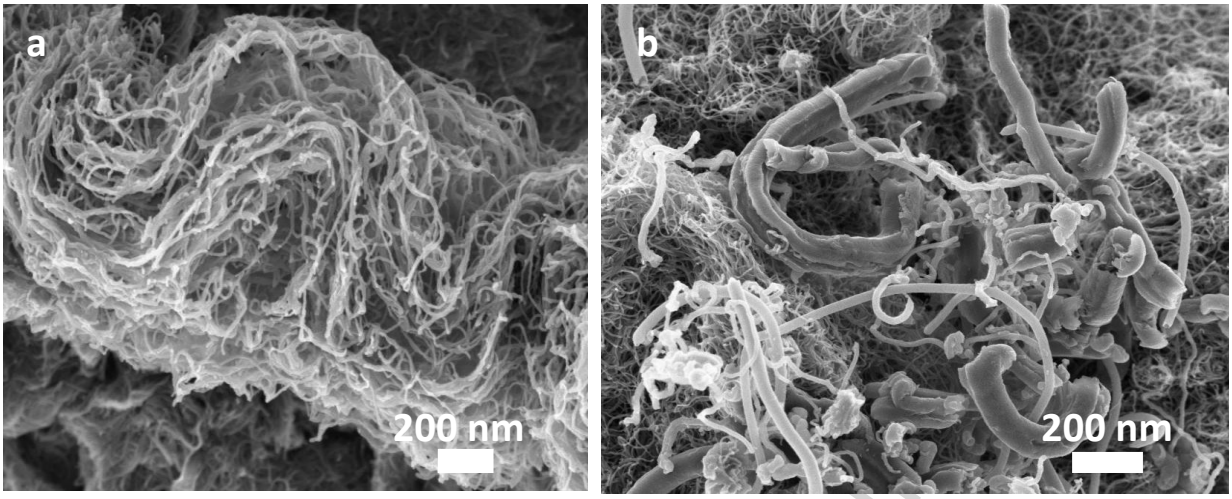

Fig 1. Field-emission gun scanning electron micrographs (FEG–SEM) of (a) MWCNTs and (b) MWCNTs-PMG

3.2. Pore surface properties

The BET surface areas and pore distributions of MWCNTs and MWCNTs-PMG were determined to investigate the changes in pore properties of the electrode.

As shown in Table 1, when discs are compacted under water, the coating of PMG onto the MWCNTs compared to pristine MWCNTs leads to a decrease of the BET surface area, the pore volume and the average pore size of the pores, respectively, from 280.5 $m^2\ g^{-1}$to 159.8 $m^2\ g^{-1}$, from 1.3 $cm^3.g^{-1}$ to 0.39 $cm^3.g^{-1}$ and from 16 to 10.5 nm.

This change is the likely result of the formation of thicker MWCNTs-PMG fibers in the MWCNTs-PMG composite, which induced a decrease of the available surface area. This observation is similar to the effect seen when chitosan and MWCTs were compacted in the presence of the same polymer in our previous work [16-18].

We further studied the integration of Nafion® as a binder in the discs, as this polymer is well-known to ensure good mechanical cohesion, to prevent electrode spalling after wetting and to have a positive impact on the stability of enzyme-based electrodes in biofuel cell applications [14, 19]. As shown in Table 1, the morphology of the material is significantly influenced by

the presence of the Nafion, which decreases the BET surface area, and the pore volumes of the pristine MWCNTs disc. In the case of the PMG- MWCNTs composite, the lower average pore of 10 nm should be beneficial for our final application by decreasing the leaching of GDH and NADP from the bioanode to the electrolyte solution. It is the reason that the synthesis of the MWCNT composite disc was performed in the presence of viscous Nafion.

Table 1: Influence of the coating of PMG onto MWCNTs on the BET surfaces area and pores sizes for different discs compacted in the presence or not of Nafion

	BET surface area($m^2.g^{-1}$)	Pore volume ($cm^3.g^{-1}$)	Average pore diameter (nm)
MWCNTs	280	1.3	16
MWCNT/Nafion	158.35	0.39	10.05
MWCNTs/PMG	159.85	0.48	12.12
MWCNTs/PMG/Nafion	52.26	0.12	9.22

This result is not consistent with the classical trend of the increase of S_{BET} with decreasing average pore size.

This observed phenomenon may be attributed to the following factors: (1) for some smaller-sized pores in the composites such as the micron scale pores, MWCNTs and their aggregates could have fully filled and occluded the pore voids, and (2) MWCNT composites could also have partly filled and covered some of the larger sized pores. Both would have the effect if decreasing the accessible pore surface for SBET.

3.2 Zeta potential

Fig 3 shows the pH dependence on the zeta potential of pristine MWCNTs and MWCNT-PMGs. Pristine MWCNTs exhibit positive zeta potentials over the whole range of pH under investigation (i.e. from 2.5 to 9.5). Such a property is related to the presence of sp2 carbons,

which favor oxonium ion adsorption as recently shown for some other carbon-based materials [23].

A different electrokinetic behaviour is observed for the MWCNT-PMG composite, which exhibits an isoelectric point slightly over 7, indicating a weaker affinity of oxonium ions towards the modified surface. MG is a basic dye (pK_a = 9.9), so it will be positively charged in pH<9.9 solution, so this indicates that its behavior as a surface layer has changed at the MWCNT-PMGs, and again different from either MWCNTs or MG monomer since the both are positively charged at pH values between 7 and 8. It can be noted, however, that both systems (pristine MWCNT and MWCNT-PMG) exhibit similar electro-kinetic behaviour at pH less than 5 (sharp increases in zeta potential), which could confirm that the MWCNTs surface is not totally covered by the PMG. In addition, there is more electro-withdrawal effect from the polymer backbone. IN fact, the measured zeta potential values may correspond to the mixed zeta potential of MWCNTs and PMG, which is in agreement with SEM observations. It is also important to note that unlike many methods used to measure the zeta potential of MWCNT composites, our method did not make use of surfactant for dispersion. Indeed, zeta potential measurement methods require the use of homogeneous CNT dispersions, since the formation of stable CNT suspensions in aqueous solution is critical for measurement. Van der Waals forces between carbon nanotubes can easily cause agglomeration and subsequent sedimentation, a major obstacle for zeta-potential measurement from electrophoretic mobility measurements.

More generally, the successful use of nanotubes for practical applications relies on the capability of breaking up bundles into individual nanotubes and keeping them in homogeneous and stable suspension. There are different, efficient, physico-chemical methods to disperse and separate nanotubes, including surfactant. Surfactant helps to individualize CNTs, even at high concentrations, and changes their wettability and adhesion behavior,

which reduces the tendency for agglomerates [26]. However, the presence of surfactants on the surface of CNTs modifies their surface properties and consequently surface charge potential.

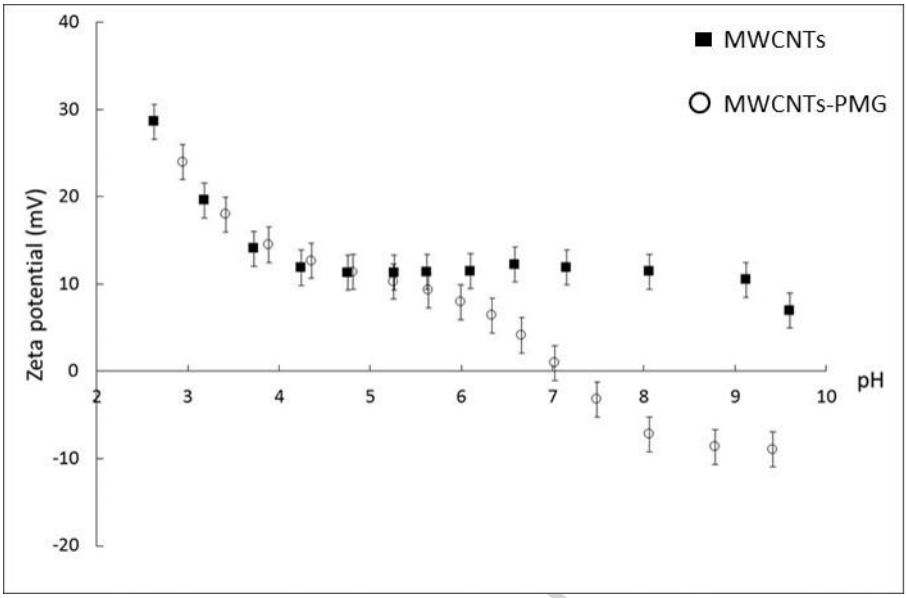

Fig 2. Variation of pristine MWCNTs and MWCNTs-PMG zeta potential as a function of pH

3.3.Electrochemical performance of the bioelectrodes

3.3.1 Flexible carbon paper based bioelectrode

The chemical polymerization of MG on the MWCNT surface was carried out using a chemical protocol derived from the works of Yasuda and Shimidzu [27] and Minteer et *al et al*. [14]. The flexible carbon paper based bioelectrode was prepared by coating a carbon porous paper with first, a MWCNT/PMG based ink, and then with a layer of GDH and NADP solubilized in a PBS buffer solution. Finally, a very thin layer of Nafion polymer was deposited in the surface to ensure the adhesion of the coated film and to prevent enzyme leaching into the solution. As shown in Fig.1, GDH catalyzes the oxidation of glucose and the reduction of $NADP^+$ to NADPH, which is then electro-oxidized on the PMG surface.

A potential window between -0.4 and 0.4 V *vs* SCE was exploited (Fig 4a) for evaluating the electrochemical behavior of the bioelectrode at pH 7,4 towards glucose oxidation. The bioanode showed a steady state catalytic current of 0.3 mA cm^{-2}. The onset potential of the glucose oxidation current was observed to be -0.2 V vs. SCE, and the current reached a steady state around 0.1 V.

In the presence of glucose in solution, the oxidation wave increases (red curve, Fig 4a) which confirms the concomitant enzymatic generation of NADPH by the MWCNT-PMG during the oxidation of glucose catalyzed by GDH. This behaviour is in agreement with results reported on the electro-oxidation of NADPH and on the capacity of PMG to regenerate NADPH [14].

The catalytic behaviour of the bioanode toward glucose oxidation was confirmed by chronoaperometry at 0.0 V *vs* SCE in stirred PBS (pH 7.4) with the appearance of an oxidation current after the addition of 15 mM of glucose in the solution.

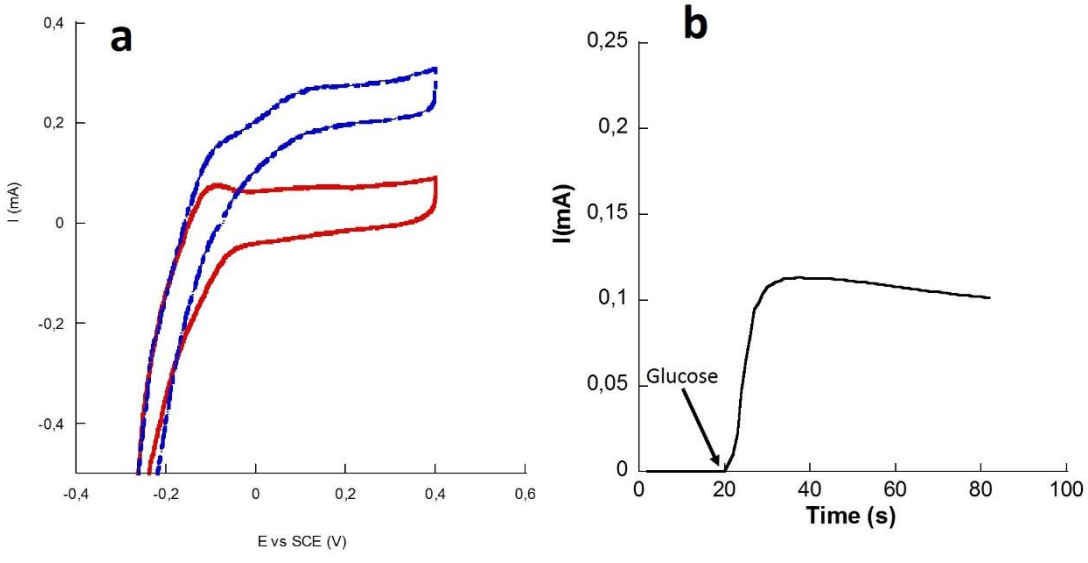

Fig 3. (a) Cyclic voltammograms of MWCNTs/PMG-NADP-GDH bioelectrode in PBS buffer solution 0.1 M pH 7.4 without (red line) and in the presence of 15 mM glucose (blue) , scan rate 5 mV/s), (b) chronoamperometric response of the bioelectrode at 0 V before and after the addition of 15 mM glucose

The stability of the bioanode was studied by periodically evaluating the stationary current of glucose oxidation obtained by chronoamperometry at 0.0 V *vs* SCE in stirred PBS (pH 7.4) in the presence of 15 mM glucose. As observed in Fig 5, the glucose oxidation current decreases substantially after few days on deployment and no glucose oxidation current is observed after one and a half days.

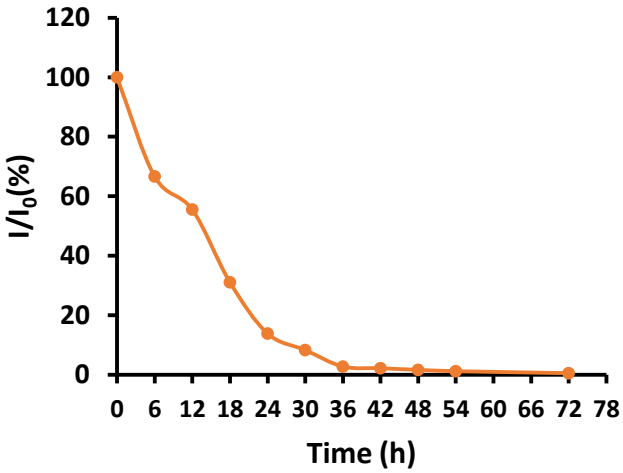

Fig 4. Stability of the oxidation current from periodic chronoamperometric measurement s at 0 V vs SCE in 0.1 M PBS (pH 7,4) with 15mM glucose.

The loss of the electrocatalytic activity of the bioanode could be attributed to different phenomena: (i) the release of the cofactor and GDH from the Nafion matrix on the surface of the electrode, (ii) the possible denaturation with time. To check the first hypothesis, spectrophotometry measurements were carried to check the presence of NADP, NADPH and GDH in the buffer solution coming from the buffer in the electrochemical cell. Table S1 (supplementary materials) shows that after one day, large amounts of NADP and NADPH are present in the buffer solution. Indeed, after 1 day around 72% of the initial amount of NADP (2.5 mg) present in the Nafion matrix was released outside the Nafion matrix, and after 3 days NADP was release, indicating that the oxidized and reduced forms of the cofactor have diffused outside the Nafion matrix. However, no trace of GDH was detected in the buffer

solution, which is in agreement with previous studies that modified porous Nafion prevents release of the enzyme [19]. These observations demonstrate that in our case, the loss of the coafactor is the limiting parameter which accelerates the reduction of the electrocatalytic activity of the bioanode with respect to the glucose oxidation. This hypothesis was confirmed by the monitoring of the activity of free GDH, that is expected to be low stable than immobilized GDH, and we can see that the free GDH keep 50% of its activity 4 days (Fig S2) confirming that the short life time of the carbon papr bioanode is mainly due to the release of the cofactor.

3.3.2 Bioelectrode based on 3D pellet

To overcome this problem, we prepared a bioanode based MWCNTs-PMG-NADP-GDH-Nafion disc fabricated by mechanical compression (chemical and material section). This method of fabrication was chosen because we observed in our previous work that this process provided a confined environment that significantly improves enzyme stabilization and minimizes the release of soluble mediators [16–18].

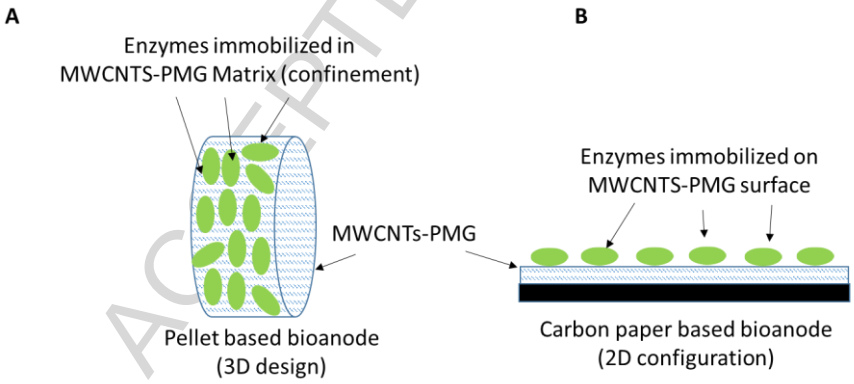

Fig 5. (A) Enzyme confined in 3D MWCNTs-PMG matric, (B) enzyme adsorbed on 2D MWCNTs-PMG surface.

In Fig 6A, a typical amperometric response curve of the bioanode disc showes the increase of oxidation current with successive additions of glucose. The bioanode achieved 90% of steady-

state current within 30 s, indicating a quick response process. The oxidation current increased from 300 µA/cm^2 to 1300µA/cm^2 after successive injections of glucose from 5 mM to 30 mM. The maximum current density of the 3D bioanode is greater than that of the 2D bioanode. However, by considering the maximum current density per mg of enzymes, the 2D bioanode delivered 0.9 mA/cm^2/mg of enzyme, 3 times more than the maximum current density of 0.3 mA/cm^2/mg of enzyme in the case of the 3D bioanode. This can be attributed to the fact that, in the case of a 2D bioanode, the enzyme layer is thinner, a few hundred µm compared to 3 mm for the 3D bioanode and, consequently, the diffusion of glucose is better in 2D bioanode compared to the 3D bioanode.

The calibration curve in Fig 6B shows a linear range from 50 µM to 20 mM glucose (y = 0,0553x - 0,0442, R^2 = 0.99) with a sensitivity of 50.8 10^{-3} A.mM^{-1}.cm^{-2} to the glucose. The deviation from linearity observed at higher glucose concentration is consistent with the K_m of the enzyme of 13.8 mM, in agreement with value reported in literature for GDH [14]. By contrast, the control (in the absence of PMG) showed that addition of glucose did not lead to increased oxidation currents, consistent with the absence of NADPH regeneration (Fig S3)

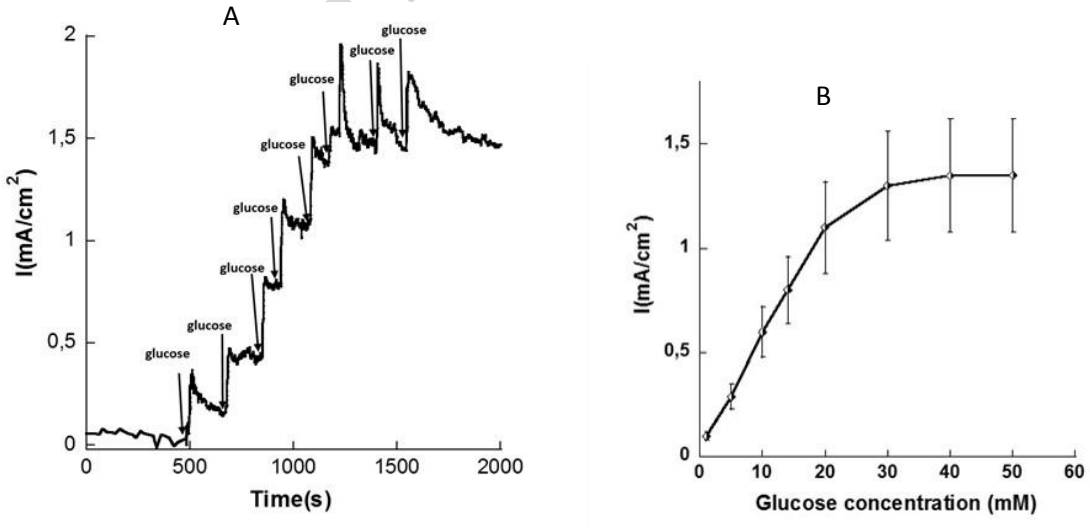

Fig 6. (A) Current-time curve of the bioelectrode MWCNTs/PMG/NADP/GDH/NAFION during successive addition of glucose (5 mM) into 0.1 M PBS (pH 7.4). Applied potential: 0.0

V *vs* SCE; (B) current oxidation response at 0.0 V *vs* SCE as a function of glucose concentration

3.3.3 The 3D bioelectrode Stability

The short-term stability of the 3D bioanode in a PBS buffer solution at PH 7.4 was evaluated by continuous chronoaperometry at 0 V (*vs* SCE during more than 80 hours (Fig 7). After a run in period during the first hours corresponding to a stabilization period, the current density reaches an equilibrium value stabilizing around 80µA cm^{-2} after 24h to at least 80 h. This suggests a favorable stability of the bio-anode and its capacity to operate stably under continuous discharge conditions at physiological pH.

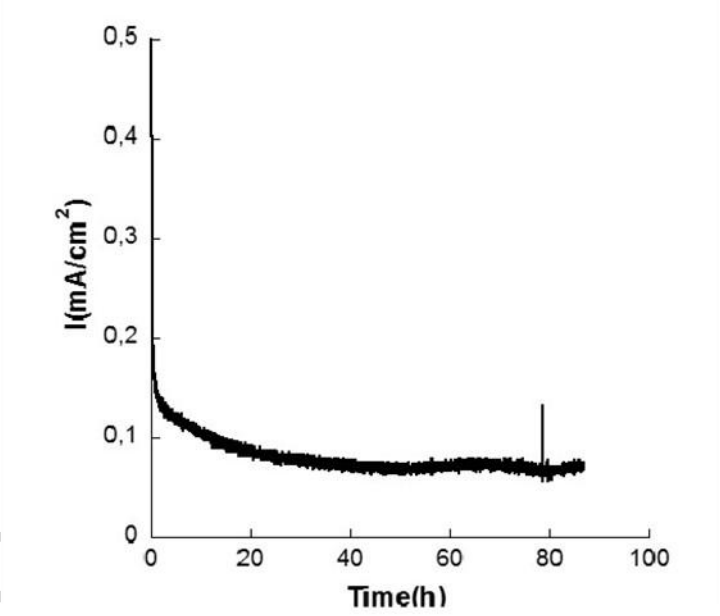

Fig 7. Current-time curve of the bioelectrode MWCNTs/PMG/NADP/GDH/Nafion evolution as function of time in physiological solution containing 5mM of glucose. Applied potential: 0.1 V *vs* SCE

We further studied bioanode long-term stability under wet storage (4°C in PBS pH 7,4) over 12 months. During this study, chronoamperometric measurements were performed under periodic discharge at 0 V during 3 hour periods of exposure to 10 mM glucose in PBS. As shown in Fig 8, during the first 2 months, the current density decreased significantly, and the bioanode lost about 60% of its initial value. Afterwards, this decrease continued, and at one year only 10% of the response was achieved.

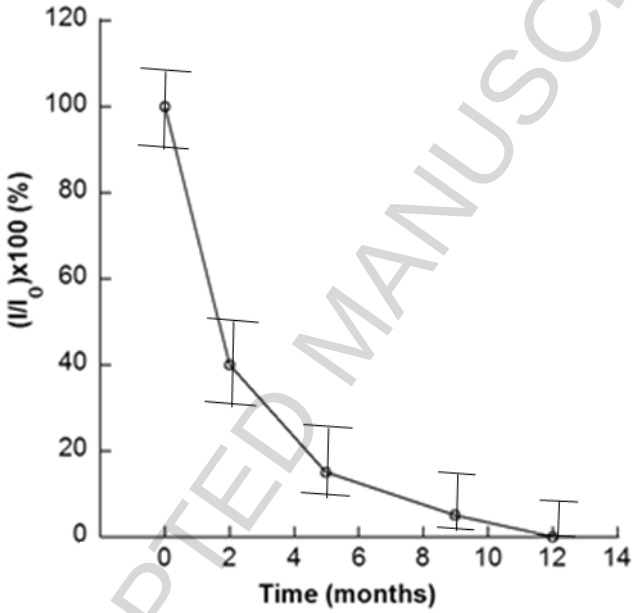

Fig 8. MWCNTs/PMG/NADP/GDH/Nafion bioelectrode stability, in PBS (pH7,4) containing 10 mM glucose, as function of time in 12 months. Applied potential: 0.0 V *vs* ECS

Fig 9A shows the chronoaperometry response toward glucose addition of a bioanode after 1-year storage and, the appearance of an oxidation current indicates residual activity. However, as shown in Fig 9B, the oxidation current density of the 10 studied bioelectrodes reaches a maximum at 20 mM glucose, where it is half the original value (Fig 7B). The lowered

apparent Km suggests loss of active cofactor leading to kinetic limitation and a lower apparent Km.

The reduced response may be due to the loss of enzyme activity or the deactivation of NADP or its release from the bioanode.

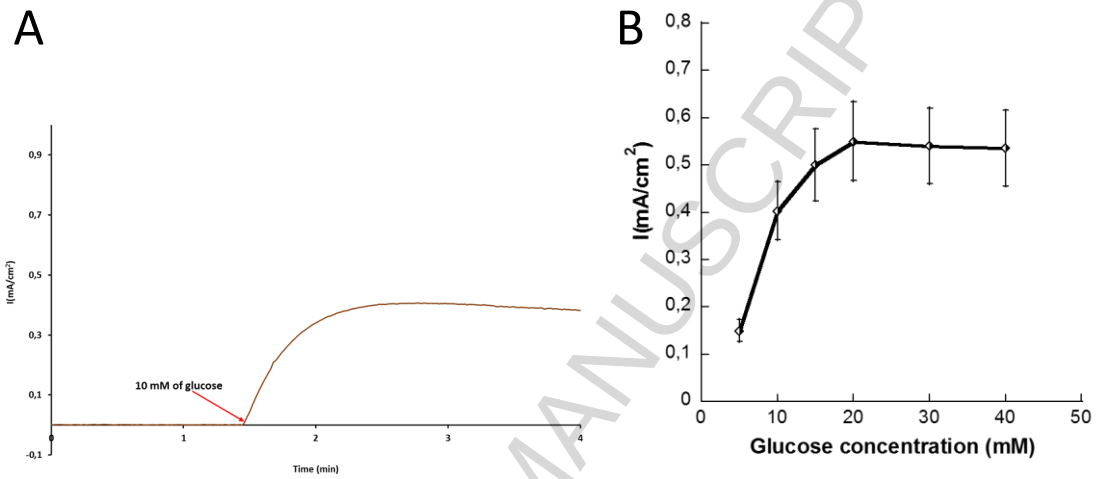

Fig 9. (A) Current-time curve of the bioelectrode WCNTs/PMG/NADP/GDH/Nafion (after 12 months) before and after the addition of 10 mM of glucose into 0.1 M PBS (pH 7.4). Applied potential: 0 V *vs* SCE. (B) Current oxidation response at 0.0 V *vs* SCE as a function of glucose concentration in 0.1 M PBS (pH 7.4) after 12 months of storage at 4°C.

To test the latter possibility, bioanodes that had lost all their electrocatalytic activity after one year were rebuilt. First, the electrical contacts of the carbon paste were removed, and then the MWCNT-PMG-GDH-Nafion composite was isolated and thoroughly ground into a powder. Finally, 20 mg of NADP were added to the powder, mixed with 100 µl of Nafion and recompressed to form new bioanode disks, electrically connected as described in section 2.3.2. The electrocatalytic activity of the reconstructed bioelectrodes was tested in the presence of 10 mM glucose at 0 V in PBS. As shown in Fig. 10 an improvement in the catalytic response was noted of only 100 $\mu A.cm^{-2}$, 7 times lower than the initial value at the

first day (Fig. 6). The reduction could be attributed to the denaturation of GDH, and also to hindered NADP diffusion within the electrode due to the presence of the Nafion matrix.

On the other hand, the presence of the electrocatalytic response demonstrates clearly that some GDH enzymes are still active after one year due to the nature of its confinement in the MWCNT-PMG-Nafion composite (Fig 10).

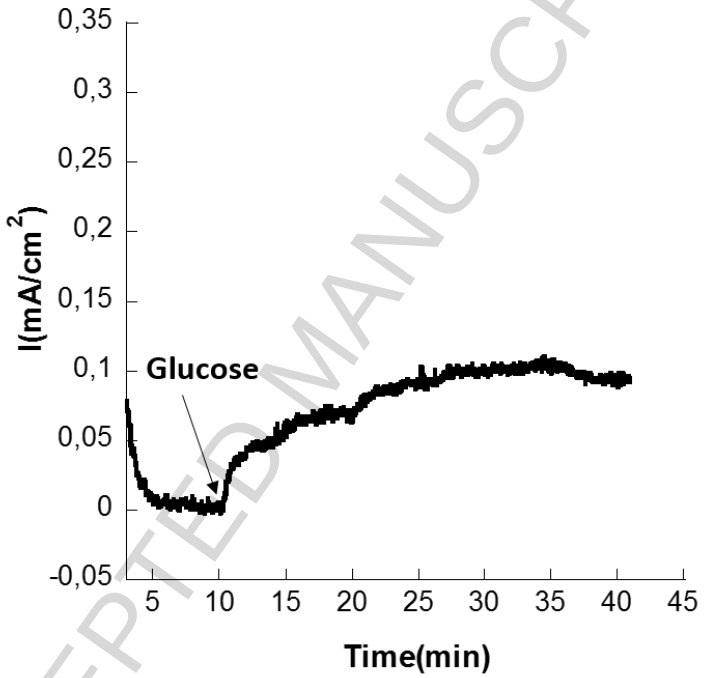

Fig 10. Current-time curve of the reconstructed bioelectrode MWCNTs/PMG/NADP/GDH/Nafion after the addition of 10mM of glucose into 0.1 M PBS (pH 7.4). Applied potential: 0 V *vs* SCE

To our knowledge, this is the first demonstration of the ability of a GDH-based bioanode to maintain electrocatalytic activity over a period of one year and thus its potential for long-term use in *in vivo* devices. In comparison, the free GDH stored in PBS buffer at 4 ° C has a stability of only one week (see Fig S3), which corresponds to a short lifetime compared to

immobilized GDH in a MWCNT-PMG matrix. Thus, it is clear that the immobilization of GDH in the MWCNTs-PMG 3D matrix is favorable to its long-term stability, which can result from different aspects: the high amount of immobilized GDH, the low releasing of GDH from the MWCNT-PMG matrix, the hydrophilic appearance of the MWCNTs-PMG surface which may imply a favorable interaction with the GDH by preventing its deactivation [28]. Furthermore, the immobilization of GDH within a porous matrix can induce confinement effects favorable to enzymatic stabilization [29, 30].

Conclusion

In this study, we described the manufacture of a new bioanode for glucose oxidation. Chemical polymerization of MG on MWCNTs provides a MWCNTs-PMG composite that can be used to catalyze the oxidation of NADPH. Indeed, the electrochemical study shows that this composite is capable of catalyzing the electro-oxidation of NADPH into NADP. In addition, the bioanode exhibits fast electron transfer and good performance against low potential (0 V) glucose oxidation. Finally, the structure of the developed bioanode is compatible with the long-term stability of GDH. This stability is attributed to the 3D MWCNTs-PMG matrix, which gives the GDH enzyme a favorable environment that considerably increases its stability. This clearly indicates that our biological device can serve as a basis for future high-efficiency glucose-based biofuel cells and could be used with other redox enzymes.

Acknowledgements

The authors thank the following organizations for financial support: The French National Research Agency (BioWatts project ANR-15-CE05-0003-01, ImABic project ANR-16-CE19-0007-03), The Auvergne Rhones Alpes program "cooperation international". The Engineering and Physical Sciences Research Council (*EPSRC*), UK.

References

[1] a) A. Zebda, C. Gondran, A. L. Goff, M. Holzinger, P. Cinquin, et S. Cosnier**,** **Mediatorless high-power glucose biofuel cells based on compressed carbon nanotube-enzyme electrodes »,** ***Nat. Commun***. 2 (2011), pp. 370

b) A. Zebda, S. Cosnier, J.P. Alcaraz, M. Holzinger, A. Le Goff, C. Gondran, F. Boucher, F. Giroud, K. Gorgy, H. Lamraoui, P. Cinquin

Single glucose biofuel cells implanted in rats power electronic devices.

Sci. Rep. 3 (2013) 1516

[2] Elouarzaki, K.; Cheng, D.; Fisher, A. C.; Lee, J.-M.

Coupling orientation and mediation strategies for efficient electron transfer in hybrid biofuel cells.

Nat. Energy, 3 (2018), pp574– 581

[3] C. Chen,, X-L. Zhao , Z-H Li, Z-G Zhu , S-H Qian and A-J. Flewitt,

Current and Emerging Technology for Continuous Glucose Monitoring

Sensors 17 (2017), pp. 1-19

[4] A. Zebda. J-P.e Alcaraz, P. Vadgama, S. Shleev, S. D. Minteer, F. Boucher, P. Cinquin, D. Martin

Challenges for successful implantation of biofuel cells, review

Bioelectrochemistry (in press)

[5] E-H Yoo and S.Y Lee

Glucose Biosensors: An Overview of Use in Clinical Practice,

Sensors 10 (2010), pp. 4558-4576

[6] S. Ferri, K. Kojima, K.

Review of Glucose Oxidases and Glucose Dehydrogenases: A Bird's Eye View of Glucose Sensing Enzymes.

J. Diabetes Sci Technol 5 (2011), pp. 1068-1076

[7] J. Moiroux, and P. J. Elving, Effects of adsorption

Electrode material, and operational variables on the oxidation ofdihydronicotinamide adenine dinucleotide at carbon electrodes

Anal. Chem., 50 8 (1978), pp 1056–1062

[8] Z. Samec and P.J. Elving

Anodic oxidation of dihydronicotinamide adenine dinucleotide at solid electrodes; Mediation by surface species

J. Electroanal. Chem., 144 (1983) 217-234

[9] P.N. Bartlett, E.N.K. Wallace

The Application of Approximate Analytical Models in the Development of Modified Electrodes for NADH Oxidation

In: R.G. Compton, G. Hancock (Eds.), Applications of Kinetic Modelling, vol. 37 (1999), pp. 35–89.

[10] Y. Ma, Z. Jin, B. Peng, J. Ding, N. Wang, and M. Zhou.

Investigation of Direct Electrooxidation Behavior of NADH at a Chemically Modified Glassy Carbon Electrode

J. Electrochem. Soc., 162 6 (2015), pp. H317-H320

[11] D. Tse, T. Kuwana

Electrocatalysis of Dihydronicotinamide Adenosine Diphosphate with Quinones and Modified Quinone Electrodes

Anal. Chem. 50 (1978), pp. 1315–1318.

[12] E.E. Ferrandi, D. Monti, S. Riva

New trends in the in situ enzymatic recycling of NADP(H) cofactors, Cascade Biocatalysis

Wiley-VCH Verlag GmbH & Co., KGaA, Weinheim, Germany (2014), pp. 23-42

[13] A. Karyakin, E. Karyakina, W. Schuhmann and H-L. Schmidt

Electropolymerized Azines: Part II. In a Search of the Best Electrocatalyst of NADH Oxidation

Electroanalysis 8 11 (1999), pp. 553-557

[14] a) M. N. Arechederra, C. Jenkins, R. A. Rincon, K. Artyushkova, P. Atanassov, et S. D. Minteer

Chemical polymerization and electrochemical characterization of thiazines for NADH electrocatalysis applications.

Electrochim. Acta, 55(2010), pp. 6659‑6664.

b) M. T. Meredith, F. Giroud, and S. D. Minteer,

Azine/hydrogel/nanotube composite-modified electrodes for NADH catalysis and enzyme immobilization

Electrochim. Acta 72 (2012), pp.. 207‑214

[15] H. Li, K. E. Worley, and S. C. Barton

Quantitative Analysis of Bioactive NAD plus Regenerated by NADH Electro-oxidation

Acs Catal. 2 12 (2012), pp. 2572‑2576

[16] S. El Ichi, A. Zebda, A. Laaroussi, N. Reverdy-Bruas, D. Chaussy, M.N. Belgacem, P. Cinquin, D.K. Martin

Chitosan improves stability of carbon nanotube biocathodes for glucose biofuel cells

Chem. Commun., 50 (2014), pp. 14535–14538

[17] S. El Ichi, A. Zebda, A. J.-P. Alcaraz, Laaroussi, F. Boucher, N. Reverdy-Bruas, D. Chaussy, M.N. Belgacem, P. Cinquin, D.K. Martin

Bioelectrodes modified with chitosan for long-term energy supply from the body

Energy Environ. Sci., 8 (2015), pp. 1017–1026

[18] S. El Ichi, J.-P. Alcaraz, F. Boucher, B. Boutaud, R. Dalmolin, J. Boutonnat, P. Cinquin, A. Zebda , D.K. Martin.

Remote wireless control of an enzymatic biofuel cell implanted in a rabbit for 2 months

Electrochim. Acta 269 (2018) 360e366

[19] S. Meredith, S. Xu, M. T. Meredith, et S. D. Minteer,

Hydrophobic Salt-modified Nafion for Enzyme Immobilization and Stabilization

J. Visualized Exp 65 (2012), e3949

[20] B. Saliha, F. Patrick, et S. Anthony

Investigating nanofiltration of multi-ionic solutions using the steric, electric and dielectric exclusion model

Chem. Eng. Sci. 64 (2009), pp. 3789‑3798

[21] P. Fievet, M. Sbaï, A. Szymczyk, C. Magnenet, C. Labbez, et A. Vidonne

A New Tangential Streaming Potential Setup for the Electrokinetic Characterization of Tubular Membranes

Sep. Sci. Technol., 39 (2004), pp. 2931‑2949

[22] A. Szymczyk, P. Fievet, et A. Foissy

Electrokinetic characterization of porous plugs from streaming potential coupled with electrical resistance measurements

J. Colloid Interface Sci., 255 (2002), pp. 323‑331

[23] L. Ginés, S. Mandal, null Ashek-I-Ahmed, C.-L. Cheng, M. Sow, et O. A. Williams

Positive zeta potential of nanodiamonds

Nanoscale, 9 (2017), pp. 12549‑12555

[24] L. Reinert, M. Zeiger, S. Suárez, V. Presser, et F. Mücklich,

Dispersion analysis of carbon nanotubes, carbon onions, and nanodiamonds for their application as reinforcement phase in nickel metal matrix composites

RSC Adv., 5 (2015), pp. 95149‑95159

[25] F. Fruscione, L. Sturla, G. Duncan, J.L. Van Etten, P. Valbuzzi, A. De Flora, E.D. Zanni, M. Tonetti

Differential role of $NADP^+$ and NADPH in the activity and structure of GDP-D-mannose 4, 6-dehydratase from two chlorella viruses

J. Biol. Chem., 283 (2008), pp. 184-193

[26] G. Gavrel, B. Jousselme, A. Filoramo, et S. Campidelli,

Supramolecular Chemistry of Carbon Nanotubes, in *Making and Exploiting Fullerenes, Graphene, and Carbon Nanotubes*, vol. 348, M. Marcaccio et F. Paolucci, Éd. Berlin: Springer-Verlag Berlin, 2014, p. 95‑126.

[27] A. Yasuda et T. Shimidzu,

Chemical and electrochemical analyses of polyaniline prepared with FeCl3

Synth. Met., 61 (1993), pp. 239‑245

[28] J. Grimaldi, M. Radhakrishna, S. K. Kumar, and G. Belfort

Stability of Proteins on Hydrophilic Surfaces

Langmuir, 31 (2015), pp 1005–1010

[29] H.-X. Zhou et K. A. Dill

Stabilization of Proteins in Confined Spaces

Biochemistry (Mosc.), 40 (2001), pp. 11289‑11293

[30] D.K. Eggers, J. S. Valentine

Molecular confinement influences protein structure and enhances thermal protein stability

Protein Sci. 10 (2001), pp. 250–261

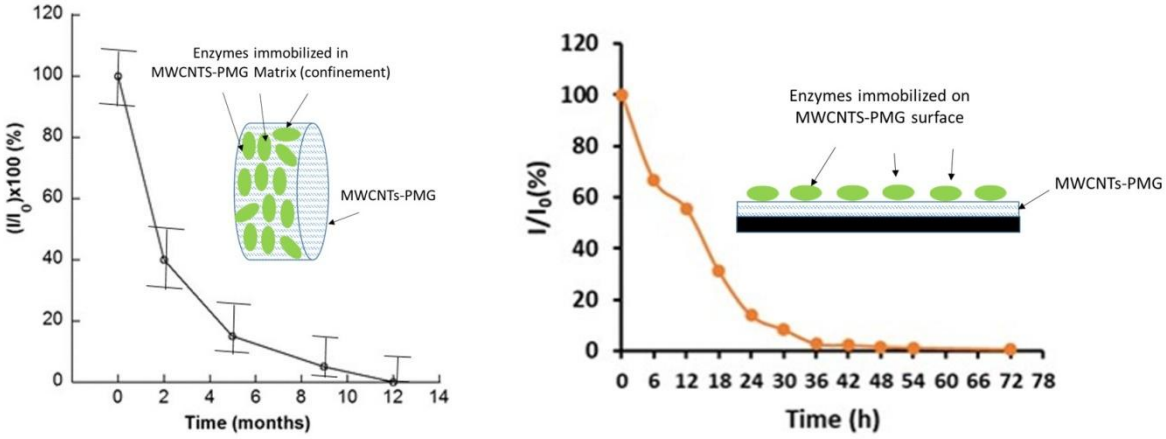

Graphical abstract